Organic & Biomolecular Chemistry

Cite this: *Org. Biomol. Chem.*, 2012, **10**, 2019

www.rsc.org/obc

PAPER

Resorcinarene bis-crown silver complexes and their application as antibacterial Langmuir–Blodgett films†

Kaisa Helttunen,[a] Negar Moridi,[b] Patrick Shahgaldian*[b] and Maija Nissinen*[a]

Received 14th November 2011, Accepted 12th January 2012
DOI: 10.1039/c2ob06920b

Silver complexes of a cation binding supramolecular host, resorcinarene bis-crown (C*N*BC5) with propyl, nonyl, decyl and undecyl alkyl chains were investigated by NMR titration, picrate extraction and single crystal X-ray diffraction. Binding studies showed that both 1 : 1 and 1 : 2 (host–Ag^+) complexes are present in solution with only a slight effect of the lower rim alkyl chain length on the binding constants (log *K* 4.0–4.2 for 1 : 2 complexes). Solid state complexes of the resorcinarene bis-crowns bearing either C_3 or C_{11} chains were obtained. Single crystal X-ray analyses showed that both derivatives bind silver ions by metal–arene and Ag···O coordination from the crown ether bridges and from the solvent, and pack in layered or bilayered fashion. Furthermore, the amphiphilic nature of C11BC5 was demonstrated using the Langmuir balance technique. Langmuir–Blodgett films of the amphiphilic C11BC5–Ag complex were transferred onto a substrate and shown to possess antibacterial activity against *E. coli*.

Introduction

Calixarenes and their close relatives, resorcinarenes, are a structurally versatile group of macrocyclic supramolecular hosts with a concave binding cavity and high affinity towards various guests, such as cations (alkali and alkaline earth metals, transition metals, ammonium ions), anions and small organic molecules.[1–3] The calixarene framework (Fig. 1) can be easily modified to enhance the binding selectivity and affinity towards cations, for example, by adding polyethylene glycol bridges to the hydroxyl groups at the calixarene lower rim or at the resorcinarene upper rim, binding pockets with tunable size and number of oxygen donors are created.[4] These compounds are called calixcrown ethers,[5] or calixarene bis-crowns[6] when two such bridges are attached to a single host, and they have proven to be very effective and selective hosts *e.g.* for caesium in nuclear waste treatment.[7] Resorcinarene bis-crown ethers[8,9] differ from the calixarene bis-crowns by confining both of the crown bridges on top of the binding cavity and having pendant alkyl groups below the binding site, forming an amphiphilic structure, whereas the calixarene bis-crowns usually exhibit 1,3-alternate conformations in the calixarene skeleton, which directs the two binding pockets to opposite sides of the molecule.

The recent rise of bacterial resistance to synthetic antibiotics and hospital-acquired bacterial infections has promoted the

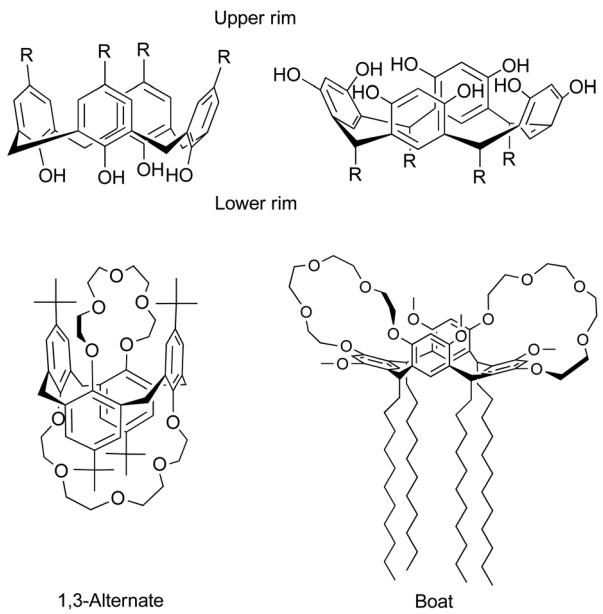

Fig. 1 Comparison of a calix[4]arene (left) with a resorcinarene (right) in the cone conformation, and a *p-tert*-butylcalix[4]arene bis-crown-5[6] with an amphiphilic resorcinarene bis-crown-5 in 1,3-alternate and boat conformations, respectively.

[a]*Nanoscience Center, Department of Chemistry, University of Jyväskylä, P.O. Box 35 Jyväskylä FI-40014, Finland. E-mail: maija.nissinen@jyu.fi; Tel: +358 50 428 0804*
[b]*School of Life Sciences, Institute of Chemistry and Bioanalytics, University of Applied Sciences Northwestern Switzerland, Gründenstrasse 40, CH-4132 Muttenz, Switzerland. E-mail: patrick.shahgaldian@fhnw.ch*

† Electronic supplementary information (ESI) available: Titration curves, Job plot, data for picrate extraction; crystallographic data and figures. CCDC reference numbers 833089 and 833090. For ESI and crystallographic data in CIF or other electronic format see DOI: 10.1039/c2ob06920b

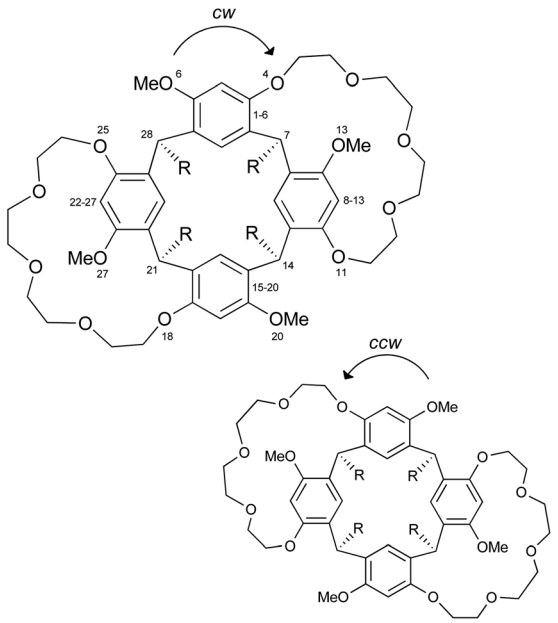

Fig. 2 General molecular formula of C*N*BC5, where N = 3, 9, 10, 11 according to the number of carbons in the alkyl group R, (R = C_NH_{2N+1}). Both clockwise, *cw*, and counterclockwise, *ccw*, enantiomers are shown.

research of alternative methods to control bacterial infections. Silver, a long known antimicrobial agent, has therefore found new applications in antibacterial materials for medical[10–14] and consumer products.[15,16] Many of these products utilize silver nanoparticles (AgNP), which provide an efficient Ag^+ release from the surface and form direct interactions with the bacterial cell wall.[13,14,17] However, silver nanoparticles also have toxic effects on mammalian cells and an extensive release of the AgNPs from the materials could lead to environmental hazards.[18,19]

Even though the exact mechanism of the antibacterial effect of silver, especially silver nanoparticles, is not fully understood, there is strong evidence that silver cations bind to the thiol groups of the proteins in the bacterial cell membrane, penetrate inside the cell and prevent normal cellular functions.[13,17,19,20] The mechanism is non-specific and therefore effective against a wide range of microorganisms. Since the toxicology and antibacterial effect of silver and AgNPs seem to depend on the particle size and the ligand,[21–24] as well as matrix and substrate properties,[25–28] there is a continuous need for new potential antibacterial materials and coatings. Several approaches have been reported; some recent examples include Ag^+ complexes,[29–32] silver clusters,[33] AgNPs with β-cyclodextrin capping,[34] electrochemically produced silver ions[35] and genetically engineered Ag^+ binding phage fibers.[36]

In supramolecular chemistry, silver complexes with macrocyclic hosts, such as crown ethers,[37] calixarenes and resorcinarenes,[38–41] and calixcrowns[42–45] are known. As a soft acid, silver prefers coordination to soft (N, S) donors,[37,40,43,44] but coordination to hard donors (O) and π-basic binding sites has also been observed.[38,39,41,42,45] However, the antibacterial activity of this kind of complex has been scarcely studied.[46] In the present manuscript, the ability of a series of resorcinarene bis-crowns to complex silver(I) in solution, in the solid-state and at the air–water interface is demonstrated. In addition, a new approach for the preparation of antibacterial coatings based on the use of self-assembled Langmuir–Blodgett (LB) films of an amphiphilic bis-crown silver complex is reported. The antibacterial properties of the LB films are assessed by applying the so-produced surface on a bacterial culture of *E. coli*.

Table 1 Binding constants for C*N*BC5:Ag^+ complexes in acetone-D6[a]

	C3BC5	C9BC5	C10BC5	C11BC5
log K_{11}[b]	2.16	2.22	2.22	2.07
log $K_{11}K_{12}$[c]	4.13	4.12	4.22	4.00

[a] NMR titration at 30 °C, *R*-values <4%, errors <8%. [b] Binding constant for the 1 : 1 complex. [c] Total binding constant for the 1 : 2 complex.

Results and discussion

Complexation studies in solution

Tetramethoxy resorcinarene bis-crown ethers, C*N*BC5's, where *N* denotes the number of carbons at the lower rim alkyl group (Fig. 2), have two polyether bridges with five oxygen donors at the resorcinarene upper rim and can thus incorporate either one or two guests into the binding site. The amphiphilic properties of the bis-crowns can be affected by selecting the length of the lower rim alkyl chains. The resorcinarene bis-crowns are known to complex alkali metal cations and silver inside their binding cavity by cation–π or metal–arene interactions and $M^+\cdots O$ coordination.[8,9,47,50] We have studied the silver binding properties of the bis-crowns (N = 3, 9, 10 and 11) in solution by means of NMR titration and picrate extraction. All of the resorcinarene bis-crowns were observed to bind silver with the affinity of log K_{11} 2.1–2.2 and log $K_{11}K_{12}$ 4.0–4.2, demonstrating that the length of the lower rim alkyl chain plays only a minor role in binding (Table 1). According to the Job plot as well as the titration data, both 1 : 1 and 1 : 2 species are present in solution. In an ideal Job plot, the maximum for the 1 : 1 complex should appear at 0.50 and for the 1 : 2 complex at 0.33. However, the obtained data show a maximum at 0.45, which can be interpreted as an indication of an equilibrium between the 1 : 1 and 1 : 2 complexes.[48]

Picrate extraction, where the transport of silver and caesium picrates from water to a chloroform phase upon complexation, was studied, and showed that the bis-crowns had a lower extraction ability towards silver (1.6–2.8%) than caesium (10%), an alkali metal cation used for reference purposes. Nonetheless, since solid liquid extraction in $CDCl_3$ showed similar complexation efficiency for both cations, the lower extraction value for silver could be explained by the differences in the cation hydration enthalpies, which are −483 kJ mol^{-1} for Ag^+ and −283 kJ mol^{-1} for Cs^+, according to Ichieda *et al.*[49]

Crystal structures

Details of the Ag^+ coordination in the bis-crown complexes were studied using single crystal X-ray diffraction. Crystals of **C3Ag2**

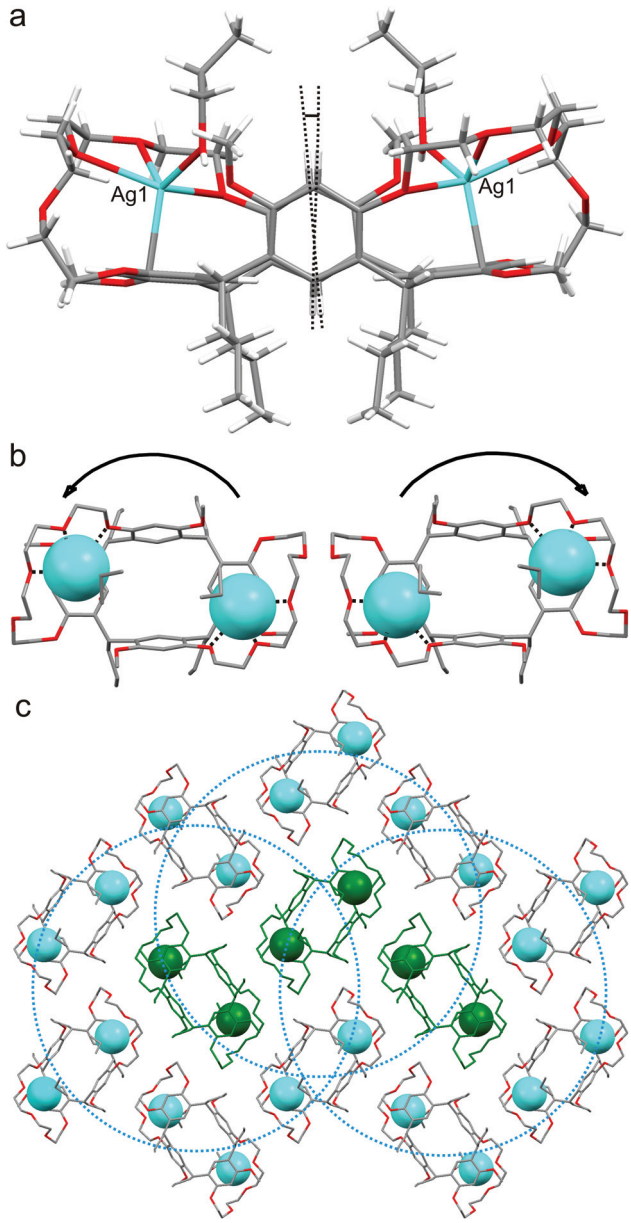

Fig. 3 Crystal structure of **C3Ag2**. (a) A side view showing tilt angle, (b) a top view of both enantiomers, (c) packing of the bis-crown complexes within a layer.

[C3BC5·$(AgPF_6)_2$·$(C_3H_8O)_2$] were grown with excess $AgPF_6$ by slow evaporation from 1-propanol, and **C11Ag1** [C11BC5·$AgPF_6$·$(C_3D_6O)_2$] with 1.5 equivalents of $AgPF_6$ from acetone-D6.

In **C3Ag2** the silver cation is coordinated by three Ag–O bonds to the crown ether bridge with bond lengths of 2.44–2.68 Å and to the 1-propanol with bond length of 2.29 Å (Fig. 3). In addition, Ag^+ is bound by a metal–arene interaction to a corner of the resorcinarene benzene ring with 2.55 Å distance to the C11 (4-position, η^1-coordination), whereas in alkali metal complexes of the bis-crowns, the cation is usually located symmetrically in the middle of the aromatic ring (η^6-coordination).[9] The cavity diameter measured as an average of the O–O distances is 6.18 Å, comparable to the silver complexes of

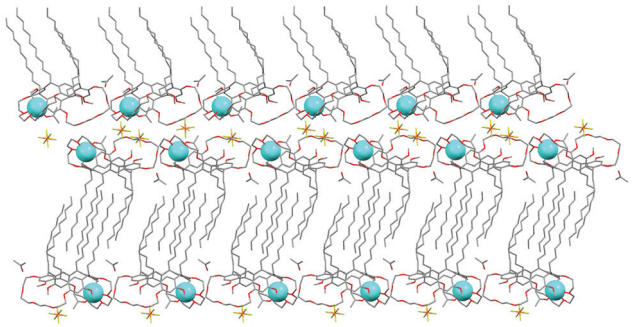

Fig. 4 Bilayer packing of **C11Ag1** with counter anions shown between the layers.

C2BC5.[47] The coordination to the other cation is identical due to symmetry. The resorcinarene core of the C3BC5 is in a slightly twisted boat conformation, which probably arises from the space needed for including the solvent inside the cavity. Interestingly, Ag^+ prefers coordination to alcohols over the PF_6^- anion, contrary to the K^+ and Cs^+ complexes, where the PF_6^- usually coordinates between the two cations inside the binding cavity.[8,9,50]

C3Ag2 packs in parallel layers, which are separated by 10.51 Å (methine carbon planes of superposed complexes). Within a layer, each complex is surrounded by six adjacent complexes with an identical chirality forming a beautiful "chain mail" pattern (Fig. 3c). The counter anions contribute to the crystal packing between the layers by forming short contacts between the crown ether bridges and the lower rim alkyl groups. Because the lower rim alkyl chains are only three carbons long, the complexes form an up-down arrangement and separation into hydrophobic and hydrophilic bilayers does not occur. The structure of **C3Ag2** is similar to the 1-propanol and 2-propanol solvates of C2BC5·2$AgPF_6$,[47] and therefore we can predict that the addition of one carbon, from ethyl to propyl, in the lower rim alkyl chains does not affect the crystal packing of the layered structures.

The amphiphilic C11BC5 crystallized as a 1 : 1 complex with silver (**C11Ag1**), where Ag^+ has very similar coordination in comparison to **C3Ag2** with the exception of acetone instead of 1-propanol as the coordinating solvent (Ag–O 2.28 Å). The silver is bound between alkoxy substituents in the 5-position of the resorcinol ring (2.37 Å) instead of the 4-position observed in **C3Ag2**, and coordinates to the three middle oxygen donors in the crown ether bridge with distances of 2.46–2.84 Å. This is probably due to the increased space at the binding pocket in comparison to **C3Ag2**, which additionally leads to a slight decrease in twisting of the resorcinarene framework. The free binding site is partly filled by a methoxy group C75 pointing inside the cavity. The long alkyl chains of **C11Ag1** pack in organized hydrophobic layers, whereas the upper rims of the complexes are placed on top of each other and connected by the anions, forming a bilayer structure clearly indicating the amphiphilic nature of the complex (Fig. 4).

Langmuir–Blodgett films

The amphiphilic self-assembly properties of C11BC5 were studied by means of the Langmuir balance technique on water or

Table 2 Langmuir isotherm data of C11BC5 on pure water and 100 μM $AgNO_3$[a]

$AgNO_3$[b]	Π_c[c]	A_c[d]	A_{lim}[e]
0	33	157	174
100	35	163	181

[a] Surface tension values are expressed in mN m^{-1} and areas in $Å^2$ per molecule. [b] In μM. [c] The surface pressure at the collapse of the monolayer. [d] The surface area at the collapse of the monolayer. [e] Extrapolation of the linear part of the isotherm on the *x* axis.

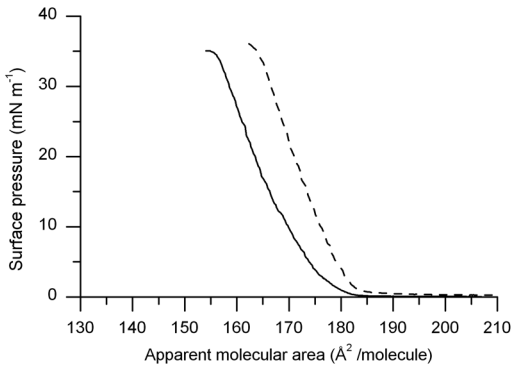

Fig. 5 *Π*/*A* isotherms of C11BC5 on pure water (—) and 100 μM $AgNO_3$ (···) sub-phases.

on an aqueous subphase containing 100 μM $AgNO_3$. From the results (in Table 2, Fig. 5) it could be seen that while the monolayer on pure water subphase collapses at 33 mN m^{-1} at a surface area of 157 $Å^2$ per molecule, the presence of silver ions causes a slight increase in the collapse pressure to a value of 35 mN m^{-1} and an increase in the collapse area to a value of 163 $Å^2$ per molecule suggesting interactions between the amphiphiles spread at the interface and the silver ions. Since the structure of C11BC5 is relatively rigid, and the resorcinarene framework is preorganized in the boat conformation for binding, no dramatic changes in the molecular areas upon complexation are expected. However, the A_c values measured are in excellent agreement with the crystal structure packing. In the solid state the pure C9BC5 shows an "apparent molecular area" of 159 $Å^2$, and C11BC5 has a collapse area of 157 $Å^2$ at the air–water interface. Moreover, the molecular area of 163 $Å^2$ at the air–water interface when the amphiphile is interacting with silver is also consistent with the solid-state packing with values of 166 $Å^2$ and 179 $Å^2$ for the 1 : 1 and 1 : 2 complexes, respectively.

Antibacterial experiments

In order to study the potential antibacterial effects of the produced complexes, four layers of the C11BC5–Ag(I) complex (*Y*-type) were transferred on hydrophobic glass substrates using the Langmuir–Blodgett approach and applied on a bacterial (*E. coli*) carpet grown on agar gel, as shown in Fig. 6. In addition to the samples, control samples with the same treatment of C11BC5 but in the absence of silver were prepared, along with controls of a glass slide dipped in 100 μM $AgNO_3$ solution and a hydrophobic glass slide. The area covered by the bacteria on the agar

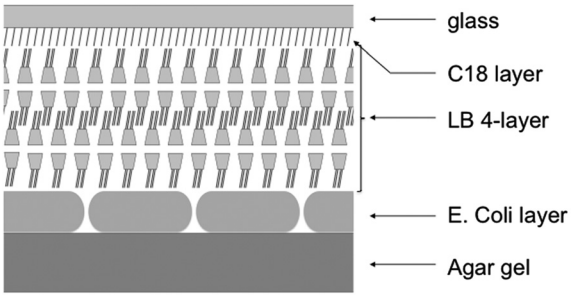

Fig. 6 Schematic representation of the experimental set-up used to test the antibacterial properties of C11BC5–Ag(I) complex.

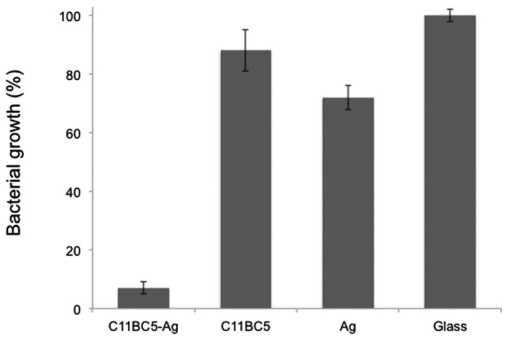

Fig. 7 *E. coli* growth (normalized results) on an agar plate submitted to a Langmuir–Blodgett multilayer of C11BC5 transferred from a subphase containing silver (100 μM, C11BC5–Ag) or pure water (C11BC5); hydrophobic glass slides (glass) and hydrophobic glass slides dipped in silver nitrate (100 μM, Ag).

gel was measured from microscope images after incubation of the samples for 5 hours at 37 °C (93%) and was used to normalize the measured data; the results are given in Fig. 7.

From the results it could be seen that the substrate dipped in silver nitrate shows only a limited loss of bacterial viability with a bacterial growth that remains as high as 72 ± 4%. This result may be attributed to the presence, at the surface of the glass slide, of unmodified areas (hydrophilic) that bind silver ions *via* electrostatic interactions and release it when in contact with bacteria. Nevertheless, the inhibitory effect observed for C11BC5–Ag(I) is relevantly higher with a bacterial growth of only 7 ± 2% while the same LB film in the absence of silver shows a growth of 88 ± 7%. This clearly shows that the antibacterial effect results from the presence of silver in the LB films. Taking into account the isotherm data and assuming the "best case" scenario where C11BC5 forms a 1 : 1 complex at the interface, the density of silver ions at the surface of the treated substrate would be approximately 0.4 nmol cm^{-2} giving a bulk concentration in the medium of 90 nM; this value is 210-fold lower than the complete inhibitory concentration (CIC) of silver for *E. coli* that has been reported to be 18.9 μM.[51]

Conclusions

The resorcinarene bis-crowns bind silver in solution, in the solid state as well as at the air–water interface on LB films. The lower

rim alkyl chain length has an effect on the self-assembling properties of the bis-crowns, as well as their complexes. When the bis-crowns are equipped with long alkyl chains (C_{11}), they show amphiphilic *i.e.* surfactant-like properties forming monomolecular Langmuir–Blodgett films, which enables their use in functional coatings. The LB films of the C11BC5–Ag complex show a relevant antibacterial effect against *E. coli* when compared to pure hydrophobic glass. The solution studies show that the binding constants for Ag^+ complexes are log K_{11} 2.1–2.2 and log $K_{11}K_{12}$ 4.0–4.2, which means that the free host, the guest, and the 1 : 1 and 1 : 2 complexes are in equilibrium and that the silver binding is reversible. Since the estimated concentration of silver in the LB films of the C11BC5–Ag complex is very low, 90 nM, it would not allow a bulk effect of the silver ions in the culture medium, but instead suggests that the antibacterial effect might be due to the close contact between the silver releasing layer and the bacteria. It is also worth noting that the antibacterial effect of silver includes a hypothesis that the Ag^+ ions bind to the thiol groups on the surface of bacteria, which is supported by the ability of the thiol-containing compounds to block the antibacterial activity of silver,[52] and that the affinity of silver for sulfur is much higher than it is for oxygen. Therefore, it is logical to assume that silver is released from the bis-crown complexes in the presence of the thiol groups on the bacterial surface, which leads to bacterial death and inhibits the overall bacterial growth as observed in these experiments. Further experiments are planned to obtain a more detailed understanding of the antibacterial effect of the bis-crown silver complexes, and whether the complex could be transported through bacterial cell membranes, enhancing the toxicity of silver. The preliminary results reported in this paper serve as a proof of principle for the development of supramolecular antibacterial materials, which in comparison to the free silver salts already show the possibility to control the release of silver and the need for lower doses. Work is underway to study the effect of thicker LB multilayers on *E. coli* growth over longer periods of time.

Experimental

Materials

All reagents and solvents were purchased from Sigma-Aldrich and VWR and used without further purification. NMR spectra were recorded with a Bruker Avance DRX 500 spectrometer at 500 MHz for ^{1}H at 30 °C. UV-vis spectra were measured using a Perkin Elmer Lambda 850 spectrometer. Tetramethoxy resorcinarene bis-crown ethers were synthesized according to a previous reference[8] from the corresponding tetramethoxy resorcinarenes.[53] Characterization data were published elsewhere.[50]

Binding studies

4 mM C*N*BC5 was titrated with $AgPF_6$ solution in acetone-D6 and ^{1}H NMR spectra were recorded after each addition at 30 °C. The shift in the aromatic resorcinarene signal at 6.005 ppm for the free host was followed and binding constants were calculated using WinEQNMR2 software.[54] Job plot samples were prepared from 4 mM solutions of C*N*BC5 and $AgPF_6$ in acetone-D6 by mixing host and guest at 9 : 1, 3 : 1, 3 : 2, 1 : 1, 2 : 3, 3 : 7, 2 : 8 and 1 : 9 ratios while keeping the total concentration constant.

Crystallography

Single crystal X-ray data were recorded on a Nonius Kappa CCD diffractometer with Apex II detector using graphite monochromated CuKα (λ = 1.54178 Å) radiation at a temperature of 173 K. The data were processed and absorption correction was made to all structures with Denzo-SMN v.0.97.638[55] unless otherwise mentioned. The structures were solved by direct methods (SHELXS-97) and refined (SHELXL-97) against F^2 by full-matrix least-squares techniques using SHELX-97 software package.[56] The hydrogen atoms were calculated to their idealized positions with isotropic temperature factors (1.2 or 1.5 times the *C* temperature factor) and refined as riding atoms. Crystal structure analysis was done using Mercury CSD 2.4 software.[57] CCDC 833089–833090.

C3Ag2: Crystallization of C3BC5 with excess $AgPF_6$ in 1-propanol by slow evaporation afforded a colorless block crystal (0.20 × 0.20 × 0.06). Orthorhombic *Pbcn*, a = 14.6967(5), b = 21.0360(7), c = 23.8819(9), V = 7383.3(4) Å^3, $C_{60}H_{84}O_{14}\cdot(AgPF_6)_2\cdot(C_3H_8O)_2$, Z = 4, D_{calc} = 1.489, FW = 1655.14, Meas. Reflns = 12333, Indep. Reflns = 6524, R_{int} = 0.0223, $R_1[I > 2\sigma(I)]$ = 0.0503, w$R_2[I > 2\sigma(I)]$ = 0.1358, GooF = 1.029. Disordered 1-propanol over two positions: (C101–C106) with site occupancy of A : B = 0.6 : 0.4. Atoms C104–C106 refined as isotropic. Disordered atoms were restrained using DFIX, DELU and SIMU.

C11Ag1: Crystallization of C11BC5 with 1.5 equiv. of $AgPF_6$ in acetone-D6 by slow evaporation afforded a colorless needle crystal (0.30 × 0.04 × 0.04). Monoclinic $P2_1/n$, a = 12.2817(4), b = 60.688(2), c = 13.4217(4), β = 97.516(2), V = 9918.0(5) Å^3, $C_{92}H_{148}O_{14}\cdot AgPF_6\cdot(C_3D_6O)_2$, Z = 4, D_{calc} = 1.245, FW = 1859.17, Meas. Reflns = 43546, Indep. Reflns = 14946, R_{int} = 0.1307, $R_1[I > 2\sigma(I)]$ = 0.0976, w$R_2[I > 2\sigma(I)]$ = 0.2245, GooF = 1.019. Absorption correction was made using SADABS.‡ C32–C38 were restrained using SADI, DELU and SIMU.

Langmuir–Blodgett films

Experiments were performed using a NIMA 112D system. The trough and the barriers were cleaned with analytical grade chloroform and nanopure water (resistivity ≥18 MΩ cm). Surface tension was monitored using a Wilhelmy plate. Compressions were performed in a continuous mode at a speed rate of 5 cm^2 min^{-1} either on pure water sub-phases or on silver nitrate aqueous solutions (100 μM). All isotherms were measured in triplicate to ensure their reproducibility. In order to ensure the absence of surface-active molecules in the sub-phase, compressions without C11BC5 spread on the surface were performed; in no case could a relevant change in surface tension be observed.

LB transfer experiments were performed using a D1L-75 vertical dipping system at a surface tension-controlled mode and a speed rate of 5 mm min^{-1}. The glass slides used as substrates for the LB deposition were cleaned by immersing them in a piranha solution (H_2O_2, H_2SO_4; 70 : 30, vol : vol)§ at 20 °C for 4 hours

followed by ultrasonic treatment in nanopure water for 30 min. The cleaned glass slides were dried under nitrogen stream and immersed in a 10 mM anhydrous heptane solution of octadecyltrichlorosilane (OTS) for 30 min at 20 °C. The glass slides were thoroughly rinsed with heptane and chloroform, respectively, and dried under nitrogen stream. Four Langmuir–Blodgett monolayers (*Y*-type) of C11BC5:Ag were transferred onto the hydrophobic glass slides at a surface tension 25 mN m^{-1}. Three controls were prepared: a hydrophobic glass slide, a hydrophobic glass slide dipped in the 100 μM $AgNO_3$ solution, and a hydrophobic glass coated with four LB monolayers of C11BC5 in the absence of $AgNO_3$.

Antibacterial experiment

Liquid LB agar (14 mL) was poured into disposable sterilized Petri dishes and allowed to solidify as thin (2.5 mm) LB agar discs. *E. coli* isolated from human intestinal florabacteria was cultivated in LB medium at 37 °C for 24 hour until reaching OD_{600} = 1. The bacterial suspension was then diluted 167 times in the LB medium. Diluted bacteria (1 mL) were deposited on the LB agar plate, spread uniformly and dried. The coated glass slides with C11BC5:Ag Langmuir–Blodgett monolayers and the three controls were gently deposited over the solidified agar gel. The prepared samples were incubated at 37 °C. The antibacterial effect was measured from the samples after a 5 hour incubation using a Olympus BX51 light microscope equipped with a 40× objective. The obtained images (6 per sample) were then analyzed using image processing software GIMP 2.6 and ImageJ in order to numerically evaluate the bacterial surface coverage. The obtained data are presented normalized using the results obtained for the unmodified hydrophobic glass slide.

Acknowledgements

This work was supported by the National Graduate School of Organic Chemistry and Chemical Biology and the FHNW research fund. We wish to thank M.Sc. Tahnie Barboza and Ms. Hélène Campos Barbosa for their assistance in the synthesis.

Notes and references

‡SADABS Area-Detector Absorption Correction, Siemens Industrial Automation, Inc., Madison, WI, 1996.
§Warning: piranha solution is highly oxidative; it could explode in contact with organics and must be handled with extreme care.

1 P. Timmerman, W. Verboom and D. N. Reinhoudt, *Tetrahedron*, 1996, **52**, 2663–2704.
2 *Calixarenes in Action*, ed. L. Mandolini and R. Ungaro, Imperial College Press, Singapore, 2000, p. 271.
3 Z. Asfari, V. Böhmer, J. Harrowfield and J. Vicens, *Calixarenes 2001*, Kluwer Academic Publishers, The Netherlands, 2001, p. 683.
4 C. Alfieri, E. Dradi, A. Pochini, R. Ungaro and G. D. Andreetti, *J. Chem. Soc., Chem. Commun.*, 1983, 1075–1077.
5 For a review of calixcrowns: K. Salorinne and M. Nissinen, *J. Inclusion Phenom. Macrocyclic Chem.*, 2008, **61**, 11–27.
6 E. Ghidini, F. Ugozzoli, R. Ungaro, S. Harkema, A. Abu El-Fadl and D. N. Reinhoudt, *J. Am. Chem. Soc.*, 1990, **112**, 6979–6985.
7 See for a review: J. Vicens, *J. Inclusion Phenom. Macrocyclic Chem.*, 2006, **55**, 193–196.
8 K. Salorinne and M. Nissinen, *Org. Lett.*, 2006, **8**, 5473–5476.
9 K. Salorinne and M. Nissinen, *Tetrahedron*, 2008, **64**, 1798–1807.
10 J. Ricco, *J. Vasc. Surg.*, 2006, **44**, 339–346.
11 M. D. Khare, S. S. Bukhari, A. Swann, P. Spiers, I. McLaren and J. Myers, *J. Infect.*, 2007, **54**, 146–150.
12 K. Galiano, C. Pleifer, K. Engelhardt, G. Brössner, P. Lackner, C. Huck, C. Lass-Flörl and A. Obwegeser, *Neurol. Res.*, 2008, **30**, 285–287.
13 H. Cao and X. Liu, *Wiley Interdiscip. Rev.: Nanomed. Nanobiotechnol.*, 2010, **2**, 670–684.
14 K. K. Y. Wong and X. Liu, *Med. Chem. Commun.*, 2010, **1**, 125–131.
15 H. Y. Ki, J. H. Kim, S. C. Kwon and S. H. Jeong, *J. Mater. Sci.*, 2007, **42**, 8020–8024.
16 T. M. Benn and P. Westerhoff, *Environ. Sci. Technol.*, 2008, **42**, 4133–4139.
17 J. Liu, D. A. Sonshine, S. Shervani and R. H. Hurt, *ACS Nano*, 2010, **4**, 6903–6913.
18 X. Chen and H. J. Schluesener, *Toxicol. Lett.*, 2008, **176**, 1–12.
19 C. Marambio-Jones and E. M. V. Hoek, *J. Nanopart. Res.*, 2010, **12**, 1531–1551.
20 N. Silvestry-Rodriguez, E. E. Sicairos-Ruelas, C. P. Gerba and K. R. Bright, *Rev. Environ. Contam. Toxicol.*, 2007, **191**, 23–45.
21 N. V. Ayala-Núñez, H. H. Lara Villegas, L. d. C. Ixtepan Turrent and C. Rodríguez Padilla, *NanoBiotechnology*, 2009, **5**, 2–9.
22 A. Le, L. T. Tam, P. D. Tam, P. T. Huy, T. Q. Huy, N. Van Hieu, A. A. Kudrinskiy and Y. A. Krutyakov, *Mater. Sci. Eng., C*, 2010, **30**, 910–916.
23 H. Liu, S. A. Dai, K.-Y Fu and S. Hsu, *Int. J. Nanomed.*, 2010, **5**, 1017–1028.
24 M. V. D. Z. Park, A. M. Neigh, J. P. Vermeulen, L. J. J. de la Fonteyne, H. W. Verharen, J. J. Briedé, H. van Loveren and W. H. de Jong, *Biomaterials*, 2011, **32**, 9810–9817.
25 A. Travan, C. Pelillo, I. Donati, E. Marsich, M. Benincasa, T. Scarpa, S. Semeraro, G. Turco, R. Gennaro and S. Paoletti, *Biomacromolecules*, 2009, **10**, 1429–1435.
26 P. Pallavicini, A. Taglietti, G. Dacarro, Y. Antonio Diaz-Fernandez, M. Galli, P. Grisoli, M. Patrini, G. Santucci De Magistris and R. Zanoni, *J. Colloid Interface Sci.*, 2010, **350**, 110–116.
27 V. Sedlarik, T. Galya, J. Sedlarikova, P. Valasek and P. Saha, *Polym. Degrad. Stab.*, 2010, **95**, 399–404.
28 X. Zan, M. Kozlov, T. J. McCarthy and Z. Su, *Biomacromolecules*, 2010, **11**, 1082–1088.
29 L. Balogh, D. R. Swanson, D. A. Tomalia, G. L. Hagnauer and A. T. McManus, *Nano Lett.*, 2001, **1**, 18–21.
30 S. Pal, E. J. Yoon, S. H. Park, E. C. Choi and J. M. Song, *J. Antimicrob. Chemother.*, 2010, **65**, 2134–2140.
31 S. Patil, J. Claffey, A. Deally, M. Hogan, B. Gleeson, L. M. Menéndez Méndez, H. Müller-Bunz, F. Paradisi and M. Tacke, *Eur. J. Inorg. Chem.*, 2010, 1020–1031.
32 C. Abbehausen, T. A. Heinrich, E. P. Abrão, C. Costa-Neto, W. R. Lustri, A. L. B. Formiga and P. P. Corbi, *Polyhedron*, 2011, **30**, 579–583.
33 I. Tsyba, B. B. Mui, R. Bau, R. Noguchi and K. Nomiya, *Inorg. Chem.*, 2003, **42**, 8028–8032.
34 S. Jaiswal, B. Duffy, A. K. Jaiswal, N. Stobie and P. McHale, *Int. J. Antimicrob. Agents*, 2010, **36**, 280–283.
35 W. K. Jung, H. C. Koo, K. W. Kim, S. Shin, S. H. Kim and Y. H. Park, *Appl. Environ. Microbiol.*, 2008, **74**, 2171–2178.
36 J. Y. Mao, A. M. Belcher and K. J. Van Vliet, *Adv. Funct. Mater.*, 2010, **20**, 209–214.
37 T. Nabeshima, *J. Inclusion Phenom. Mol. Recognition*, 1998, **32**, 331–345.
38 A. Ikeda and S. Shinkai, *J. Am. Chem. Soc.*, 1994, **116**, 3102–3110.
39 W. Xu, R. J. Puddephatt, K. W. Muir and A. A. Torabi, *Organometallics*, 1994, **13**, 3054–3062.
40 A. F. Danil de Namor, O. E. Piro, L. E. Pulcha Salazar, A. F. Aguilar-Cornejo, N. Al-Rawi, E. E. Castellano and F. J. Sueros Velarde, *J. Chem. Soc., Faraday Trans.*, 1998, **94**, 3097–3104.
41 M. Munakata, L. P. Wu, T. Kuroda-Sowa, M. Maekawa, Y. Suenaga, K. Sugimoto and I. Ino, *J. Chem. Soc., Dalton Trans.*, 1999, 373–378.
42 P. Thuéry, M. Nierlich, F. Arnaud-Neu, B. Souley, Z. Asfari and J. Vicens, *Supramol. Chem.*, 1999, **11**, 143–150.
43 J. Y. Lee, J. Kwon, C. S. Park, J. Lee, W. Sim, J. S. Kim, J. Seo, I. Yoon, J. H. Jung and S. S. Lee, *Org. Lett.*, 2007, **9**, 493–496.
44 J. Y. Lee, H. J. Kim, C. S. Park, W. Sim and S. S. Lee, *Chem.–Eur. J.*, 2009, **15**, 8989–8992.
45 M. S. Wong, P. F. Xia, P. K. Lo, X. H. Sun, W. Y. Wong and S. Shuang, *J. Org. Chem.*, 2006, **71**, 940–946.
46 Y. Yi, Y. Wang and H. Liu, *Carbohydr. Polym.*, 2003, **53**, 425–430.

47 K. Salorinne, O. Lopez-Acevedo, E. Nauha, H. Häkkinen and M. Nissinen, *CrystEngComm*, 2012, **14**, 347–350.
48 V. M. S. Gil and N. C. Oliveira, *J. Chem. Educ.*, 1990, **67**, 473–478.
49 N. Ichieda, M. Kasuno, K. Banu, S. Kihara and H. Nakamatsu, *J. Phys. Chem. A*, 2003, **107**, 7597–7603.
50 K. Helttunen, K. Salorinne, T. Barboza, H. Campos Barbosa, A. Suhonen and M. Nissinen, *New J. Chem.*, 2012, DOI: 10.1039/c2nj20981k.
51 G. Zhao and S. E. Stevens Jr, *BioMetals*, 1998, **11**, 27–32.
52 S. Y. Liau, D. C. Read, W. J. Pugh, J. R. Furr and A. D. Russell, *Lett. Appl. Microbiol.*, 1997, **25**, 279–283.
53 M. J. McIldowie, M. Mocerino, B. W. Skelton and A. H. White, *Org. Lett.*, 2000, **2**, 3869–3871.
54 M. J. Hynes, *J. Chem. Soc., Dalton Trans.*, 1993, 311–312.
55 Z. Otwinowski and W. Minor, *Methods Enzymol.*, 1997, **276**, 307–326.
56 G. M. Sheldrick, *Acta Crystallogr., Sect. A: Found. Crystallogr.*, 2008, **64**, 112–122.
57 C. F. Macrae, I. J. Bruno, J. A. Chisholm, P. R. Edgington, P. McCabe, E. Pidcock, L. Rodriguez-Monge, R. Taylor, J. van de Streek and P. A. Wood, *J. Appl. Crystallogr.*, 2008, **41**, 466–470.